We thank the reviewer for his/her thoughtful and constructive questions and suggestions on our manuscript, which will improve the clarity and the quality of the paper.

Comments 1:

8-9 I suggest that the authors remove the reference to CaCO3 export from the surface ocean. In the ocean, sinking velocities are greatly complicated by flocculation with organic matter, and through grazing - as mentioned in line 178, most coccoliths probably ended up in sediment packaged up in larger aggregates such as faecal pellets. It would be useful however to have the complexities of the real ocean alluded to much more clearly and earlier in the manuscript, so that readers are not tempted to use these calculations to estimate export rates directly from individual coccoliths in sediment.

Reply: Agreed. We have removed the reference as your suggestion.

Comments 2:

24-38 From a non-specialist point of view it is not clear from the first paragraph why it is desirable to obtain monospecific fractions.

Reply: Thank you, we have tried to clarify this. Published data show that coccoliths have strong species and/or size-species vital effects in oxygen and carbon isotope and in elemental ratios (e.g. Ziveri et al., 2003; Rickaby et al., 2007; Stoll et al., 2012; Hermoso et al., 2016; Mejia et al., 2018). To be able to glean useful information from the geochemistry of fossil (or water sample) coccoliths, it is therefore desirable to try to separate monospecific or size-restricted fractions, which will provide more precise information on the past environment than a mixed coccolith fraction. We have added this in the new manuscript version.

Comments 3:

Eq. 2-2 test this equation in an ideal scenario using glass spheres?

Reply: Thank you for your suggestion. However in the context of our study, we think the principle of the (theoretically-derived) equation is clear and it is not necessary to design a new experiment to prove it.

Comments 4:

150 This doesn't make sense

Reply: We are not sure of the source of confusion. Please clarify this comment.

Comments 5:

89-119 I think this section would benefit from being slightly more thorough and clear about how the proposed protocol is actually implemented. For example: I assume that when counting coccoliths in the lower part of the settling vessel, that the remaining suspension must be homogenized, including re-suspending any coccoliths that have settled out, before counting. If so, this should be stated explicitly.

Reply: Constructive suggestion. Your guess is correct and we have added some more descriptions on this measurement (Lines 101-119).

Comments 6:

a) 162-164 “sediments accumulating in the lower suspension, the particle concentration can be more than 4 times higher than the initial homogenous concentration” – This is important and should be discussed thoroughly. How do these higher concentrations arise? Presumably due to the size range of coccoliths in the sample. Can this effect be described quantitatively as a function of the standard deviation of coccoliths sizes in the initial sample?
b) Figure 2 This figure doesn’t really represent the assumptions made by the authors. For coccoliths of a given size, the boundary between the suspension and the supernatant is infinitely sharp, and the suspension does not change in density – but rather there is a build up of coccoliths deposited on the bottom of the vessel. In a mixed species assemblage, or where coccoliths are a range of sizes, then the suspension will become more dense towards the bottom over time as shown here, but this isn’t currently represented in the equations (or at least not clearly!). For this reason, these coccolith images are fairly unhelpful. A schematic figure that more clearly shows the change in coccolith density might be better, with a more obvious range in sizes (or not).

Reply: These two comments are talking about the same issue: “Will the coccolith concentration be higher in the lower suspension during the settling?” and “if so, what caused this phenomenon?” We can share our experience and try to explain these to you.

We don’t think the variations of coccolith shape can cause a significant increase of sediment concentration in the lower suspension (it can, but it is not significant). This is because we have pre-separated coccoliths from sediment before measurement and the coccoliths were not in a wide size range. The concentration of suspension really increased in some situations and could be seen with naked eyes. This often happened when we used centrifuge tubes. We observed the sediment concentration increased at the depth where the shape of vessel narrowed. So we think this phenomena was caused by the friction of the vessel wall and collision between particles. Precisely calculation this process is too complex and beyond the scope of paper. Importantly, because we only pump out the upper suspension in each vessels, the raise of concentration around bottom has not affected our result. We have added a new sentence in Lines 185-186 to avoid misunderstanding.

We made a mistake in original Figure 2, in which the sediment concentration variation had been overstated. We have redrawn this figure to correct this. We sincerely appreciate your carefully reviewing.

Comments 7:

“confirming the fact” is far too strong. It is true that these numbers are consistent

Reply: We have changed confirming to suggesting (Line 202).

Comments 8:

Why is H. carteri excluded?

Reply: Thanks for pointing out that this needs clarification. We didn’t use *H. carteri* in the regression because of its specific shape, which is quite different to the other species studied. This was explained it in Lines 224-233 (Lines 203-205 in the former version): the ellipticity of *H. carteri* (~0.6) is significant lower than other coccolith (among 0.8-0.9), therefore its settling behavior differs from other species. This is also illustrated in Figure 6d and Figure C3. We have reorganized this part to make it clearer.

Comments 9:

a) I assume that the asymmetrical uncertainties on sinking velocity may arise due to an assumed normal distribution of coccolith size via the quadratic relationship? If so, this should be stated.
b) Appendix E It's not clear to me how a Monte Carlo approach has been used here, nor the benefits of using such an approach over propagation of uncertainty equations. As far I understand it, the authors have simply calculated the uncertainty associated with equation 2-1, for a range of explicit values of N1 and N2.

Reply: These comments are about the error estimation and we reply to them together.

We suggested that difference in uncertainties was caused by the error of R_{cal} (Figure 5) and coccolith shape distributions were never involved in the sinking velocity calculation. In Figure 5, the positive direction error bars are often larger than negative ones and we think this was caused by the Poisson distribution of uncertainty in coccolith counting. So when we do the regression (this regression was also a Monte Carlo process), we will find the uncertainty of slope (sinking velocity=-10*slope) is asymmetric. That is the source of asymmetrical uncertainties.

The Monte Carlo method is a common method for error propagation and is suitable for our study for three reasons. Firstly, no matter how complex the target equation is, what we need to do is choose the right error distributions for some independent variables, by running the code and collecting the results. This can save a lot of time compared with partial differential equation derivation.

Secondly, traditional error propagation assumpts that all uncertainties have a normal distribution. However, as we describe in Appendix E, the error distribution of coccolith counting is a Poisson distribution. Although when the number is large enough the Poisson distribution can be treated as normal distribution, in our study, there were only around 10 coccoliths or even less in many FOVs and we input each FOV data independently. So we think the Monte Carlo method with exact error distribution is more suited to our data.

The last reason is that if we use the Monto Carlo method, we can take full advantage of uncertainty in the regression process. Otherwise, the liner regression will not consider the distribution of uncertainties of the input data in a single regression and we will lose information related to coccolith counting errors. That is why we employed the Monte Carlo method for error propagation rather than using the partial differential equations.

In the revised version, we have reorganized the Appendix E to clarify how we did the Monte Carlo process (Line 587-591). Because the method is a common one, we don't think it is necessary to explain all of the above in the paper.

Comments 10:

If the authors are using the volume and sinking distance to estimate the average

vessel diameter, the equation given in the caption doesn't look right. I think it should be:

Reply: Thank you for pointing out this mistake. We have checked the original equation in excel to make sure the calculation results are based on the correct formula.

Comments 11:

Appendix D: While the math seems sensible, I found it difficult to follow this derivation despite its simplicity. Nevertheless, the way of measuring sinking velocity proposed here is interesting, and I would personally prefer to see its derivation in the main text rather than the appendix.

Reply: Thank you for this suggestion. We have discussed this among co-authors. In previous versions, these derivations were indeed in the main text. We moved them to the appendix for a smoother reading experience. For those who wants to see details, they can check the appendix. So we want to keep them in the appendix and we have tried to make every equation clearer. If there are still some discontinuities in logic, please let us know.

Comments 12:

Each variable should be defined after it is first used throughout the text, and again within the appendix if this is to constitute a stand alone derivation. A single symbol would be better for sinking velocity unless either 's' or 'v' is subscripted.

Reply: Thank you for this suggestion. We have redefined the symbol, such as turning sv to v and V1 to V_1.

Comments 13:

a) The authors justify the assumption that settling rates are approximately constant with a time course analysis of Gephyrocapsa oceanica, concluding that for the first 4 hours, settling velocities do indeed appear to be constant. Is this period of 4 hours applicable across coccoliths of other size and shape? What causes the deviation from the ideal stokes law behaviour after 4 hours? If this were an ideal scenario, the top part of the vessel should be completely devoid of coccoiliths of a given size after a period of time T, where T = D sv .
b) If sv is a function of t, show this. If not, and you're interested in the average sv, I think
c) Figure D1: What does Monte Carlo mean in b) here? Have the parameters of the model been fitted to the data points multiple times, resampling their values from an assumed distribution? If so, the spread of constrained these values rather than just the average needs to be plotted to show how uncertain this relationship is. I assume that the early, straight part of the line in b) is the part that is described by equation 2-2, before the settling velocities decrease when the suspension is left for 4 hours (d) - if so, it would be helpful to plot this straight line on here too and label it as the fit to equation 2-2 in the valid region. I don't understand how the authors obtain the shape of the relationship in b), so would benefit from further explanation. Why are there more data points in d) than in b)?

Reply: These questions concern the assumption "we treated the average sinking velocities as the sinking velocities of the coccoliths with the average length" in lines 138-140 and its proof in Appendix D.

Actually, the average sinking velocity is a function of t and that is why the modeled R_{cal} and instant sinking velocity deviated from the ideal stokes law behaviour after 4 hours. The fundamental reason is that the average coccoliths length in the suspensions decreases slightly with settling time (see the Figure D1-c). But as proved in Appendix D, this variation won't draw significant influence on our velocity result. To be honest, we don't know the exact function neither know how to calculate it. In this study, we used a threshold of R_{cal}=15% to avoid variations in the average sinking velocity with coccolith size dynamics (this has been described in Appendix D of the former version). Only one data point of small *Ca. leptoporus* in our dataset was significant smaller than 15% (~5%). We think it is interesting to discuss the relationship between average sinking velocity and time, but this topic is beyond the scope of this study and perhaps also beyond our experiment conditions.

Your guess about a certain size of coccoliths vanishing from the upper column is correct and that's the principle of coccolith separation by settling method. We did not descript the protocol details because we do not present a fundamentally new protocol for separation in this study. If we know two coccoliths' sinking velocities and their difference is large enough, we can chose the settling duration easily by T=D/v, where v is the larger sinking velocity between the two kind of coccoliths. But as all reviewers' suggest, we have added this brief description in the last part of the main text.

For the Monte Carlo method here, we resampled the coccolith length from the assumed length distribution but this process is a little difference from typical Monte Carlo simulation. Because we only used the resampling dataset for a one-time simulation and did not repeat the simulation many times (we can do repeat simulations but the result can hardly fully plotted on this figure because of huge data amount). So, we have removed the term 'Monte Carlo' to avoid misleading readers. Moreover, we have added more descriptions for this simulation in Lines 537-540.

We have redrawn Figure D1 adding the fitting results in D1-b following your suggestion. We think the new figure can illustrate the statement 'we can assume the average sinking velocity as the sinking velocity of the the coccoliths with the average length' better. Thank you for this suggestion.

The points in Figure D1-b are what we measured in experiments and those in Figure D1-d are from simulations. We have explained this in Lines 561-563.

Comments 14: The ratio given in line 458 is not the number of coccoliths in a thickness dD as stated - as the authors have defined here, it is the number of coccoliths per unit unit thickness.

Reply: We have added a statement "dD is unit thickness".

Comments 15:

a) 482 equation 2-6 doesn't exist. Should this be D-6?
b) eq. D-6 This is difficult to follow. Keep equation in symbol format before introducing numbers
c) eq. D-7 What is -10, and what is k?

Reply: Yes. Equation 2-6 should be D-6 and we have rewritten equation D-6 following your suggestion.

In equation D-7, 'k' is the slope of R_{cal} against T. We defined it just above this equation in Line 547 (Line 484 in former version). If we use V_1=15 ml, V_2=10 ml and D=6 cm, the equation D-5 will be:

$$\mathrm{R} = \frac{3}{5} - \frac{v}{10} \times t \qquad \text{(eq. 1)}$$

Here R is equal with R_{cal}, v is sink velocity and t is time. The slope of R-t, marked as k, is '-v/10'. This process was done just for a simplification of calculation and making our raw data more comparable and clearer as described in Line 539-544.

Comments 16:

Firstly, all coccoliths belong to a particular species are assumed to sink at exactly the same rate. Secondly, they are assumed to sink at a constant velocity from the instant that the suspension is left. I would like to see a calculation in the appendix estimating the time and distance that a particle falls before it reaches terminal sinking velocity, to show whether or not it is justifiable to ignore the accelerating phase for all of the particle sizes considered here. Intuitively I imagine this is a fair assumption, but it would be nice to see in numbers.

Reply: We did not assume all coccoliths to sink at same rate. Our assumptions are two parts: (1) the sinking velocity we measured is the average sinking velocity of all coccoliths of a certain species; (2) the average sinking velocity can represent the sinking velocity of coccolith with a mean length for that species. This assumption has been stated in Lines 135-140. However, we failed to explain the proof clearly in Appendix D, so we have illustrated this in the **reply** to **Comments13** and improved it.

For your second questio, let us do some simple calculations to prove it. Because coccolith hydrodynamics is too complex to be calculated accurately, we take a calcite sphere as an example to show how fast can it reach terminal speed. Here we use the term 'terminal speed' to describe the speed when coccoliths sink in force balance.

If we chose downward force or speed as positive, the movement of a calcite sphere can be described by Newton's second law as following equation:

$$\mathrm{F} = \frac{4}{3}\pi r^3 \rho_{cal} g \; - \frac{4}{3}\pi r^3 \rho_{water} g - 6\pi\eta r v = \frac{4}{3}\pi r^3 \rho_{cal} \frac{dv}{dt} \qquad \text{(eq. 2)}$$

Where F is the resultant of force, *r* is sphere radium, ρ_{cal} is the density of calcite (2.7 g cm^{-3}), ρ_{water} is the density of water (~1.0 g cm^{-3}), η is the viscosity of water, *v* is sinking velocity of sphere. The second term of eq.2 is gravity, the third one is buoyancy, the next one is drag force and the term in the left of second equal sign is the sphere mass multiplied by accelerated speed. The eq. 1 can be modified to the following form:

$$\frac{dv}{dt} = \; -\frac{9\eta}{2r^2} v + \frac{g}{\rho_{cal}} (\rho_{cal} - \rho_{water}) \qquad \text{(eq. 3)}$$

We can simply the equation as following:

$$\frac{dv}{dt} = \; av + b \qquad \text{(eq. 4)}$$

where a, b and c are as following

$$\mathrm{a} = -\frac{9\eta}{2r^2} \qquad \text{(eq. 5)}$$

$$\mathrm{b} = \frac{g}{\rho_{cal}} (\rho_{cal} - \rho_{water}) \qquad \text{(eq. 6)}$$

$$\mathrm{c} = \ln b \qquad \text{(eq. 7)}$$

Solve the differential equations with an initial value $v_{t=0}$=0, we can get:

$$\mathrm{v} = \frac{e^{(c+at)} - b}{a} \qquad \text{(eq. 8)}$$

So the sinking velocity, v, as a function of sinking time, t, can be written as following equation:

$$\mathrm{v} = \frac{-e^{\left[-\frac{9\eta}{2r^2}t + \ln\left(-\frac{g}{\rho_{cal}}(\rho_{cal}-\rho_{water})\right)\right]} + \frac{g}{\rho_{cal}}(\rho_{cal}-\rho_{water})}{\frac{9\eta}{2r^2}} \qquad \text{(eq. 9)}$$

Ignoring other parameters, if we set the time, 't', to large enough (or we can say infinite mathematically), we can get the terminal speed (marked as v_t), which is exactly same as the Stocks' law:

$$\lim_{t\to\infty} \mathrm{v} = \frac{2(\rho_{cal}-\rho_{water})gr^2}{9\eta} \qquad \text{(eq. 10)}$$

But actually, *v* can equal to v_t even when t is a quite small number. We can see the term, $e^{(c+at)}$, in eq. 7 will be close to zero when a*t is negative shifting. If we set *r* varies between $1*10^{-6}$m to $1*10^{-5}$m (typical coccolith size), *a* will be ~-10^9, while c is only about 1.8. As long as, *t* is close to 10^{-7} s, the exponent term will be almost close to zero (e.g. $\exp(-10^2)=3.7*10^{-44}$) making the sinking velocity equals to balance velocity. This value ($t=10^{-7}$ s) is about 11-12 order of magnitude smaller than the time we discuss in our paper. So the assumption that coccolith can reach the terminal speed fast is reasonable. We believe that it is not essential to include the above derivation in the manuscript, following the articles about particles settling cited in our manuscript.

Comments 17:

I would like a more in depth discussion of these features and other factors affecting sinking velocities in the lab - for example - temperature gradients leading to convection, entrainment of small particles by larger ones (i.e. do smaller coccoliths sink faster when there are large coccoliths present?).

Reply: Good suggestions. We never considered the convection caused by temperature gradients. Because one of the foundations of this experiment is all coccoliths sinking velocities are in still solutions. In settling, there is no temperature gradient and no evidence for convection. Because the solution temperature is homogeneous and constant during the experiment.

There has been a lot of papers discussing a multi-species particles in hindering settling. In Masliyah's calculation (1979), the velocities of smaller particles only decrease significant when the volume of particles excess 10%. In our experiments, the volume of sediments are controlled below 5%. And there is another study calculating the different size particles with same density in a hindering settling process (Greenspan and Ungarish, 1982). However, we think such a discussion is beyond our study's scope.

References:

Greenspan, H. P., and M. Ungarish. "On hindered settling of particles of different sizes." International Journal of Multiphase Flow 8.6 (1982): 587-604.

Masliyah, Jacob H. "Hindered settling in a multi-species particle system." Chemical Engineering Science 34.9 (1979): 1166-1168.

Stoll, Heather, et al. "B/Ca in coccoliths and relationship to calcification vesicle pH and dissolved inorganic carbon concentrations." Geochimica et cosmochimica acta 80 (2012): 143-157.

Rickaby, R. E. M., et al. "Coccolith chemistry reveals secular variations in the global ocean carbon cycle?." Earth and Planetary Science Letters 253.1-2 (2007): 83-95.

Ziveri, P., et al. "Stable isotope 'vital effects' in coccolith calcite." Earth and Planetary Science Letters 210.1-2 (2003): 137-149.

Stoll et al., 2012; Hermoso et al., 2016; Mejia et al., 2018).

A refinement of coccolith separation methods: Measuring the sinking characters of coccoliths

Hongrui Zhang[1, 2], Heather Stoll[2], Clara Bolton[3], Xiaobo Jin[1], Chuanlian Liu[1]

[1] State Key Laboratory of Marine Geology, Tongji University, Shanghai, 200092, China

[2] Geological Institute, Department of Earth Science, Sonneggstrasse 5, ETH, 8092, Zürich, Switzerland

[3] Aix-Marseille Univ, CNRS, IRD, Coll de France, CEREGE, Aix en Provence, France.

Correspondence to: Chuanlian Liu (liucl@tongji.edu.cn)

Abstract. ~~The~~ Quantification sinking velocities of individual coccoliths ~~are relevant~~will contribute to ~~for export of their CaCO3 from the surface ocean, and for~~ optimizing laboratory methods ~~to~~ for separating~~e~~ coccoliths of different sizes and species for geochemical analysis. ~~In the laboratory, t~~The repeat settling/decanting method was the earliest method proposed to separate coccoliths from sediments ~~for geochemical analyses~~, and is still widely used. However, in the absence of estimates of settling velocity for non-spherical coccoliths, previous implementations have depended mainly on time consuming empirical method development by trial and error. In this study, the sinking velocities of coccoliths belonging to different species were carefully measured in a series of settling experiments for the first time. Settling velocities of modern coccoliths range from 0.154 to 10.67 cm h^{-1}. We found that a quadratic relationship between coccolith length and sinking velocity fits well and coccolith sinking velocity can be estimated by measuring the coccolith length and using the length-velocity factor, k_{sv}. We found a negligible difference in sinking velocities measured in different vessels. However, an appropriate choice of vessel must be made to avoid 'hindered settling' in coccolith separations. The experimental data and theoretical calculations presented here ~~will~~ support and improve the repeat settling/decanting method.

Style Definition: Heading 4: Left

1. Introduction

Coccolithophores are some of the most important phytoplankton in the ocean. They can secrete calcareous plates called coccoliths, which contribute significantly to discrete particulate inorganic carbon in the euphotic zone and to $CaCO_3$ fluxes to the deep ocean (e.g., Young and Ziveri, 2000; Sprengel et al., 2002). , ~~and~~Coccolith morphyology, geochemisity and fossile assemblage composition can reflect ~~record~~ paleoenvironmental changes (e.g., Beaufort et al., 1997; Stoll et al., 2002; Zhang et al., 2016). However, the use of coccolith geochemical analyses in paleoenvironmental reconstructions ~~is~~ was so far hindered by the difficulty of isolating coccolith compared with foraminifera. Two main methods have been developed to concentrate near-monospecific assemblages of coccoliths from bulk sediments: one is the method based on a decanting technique (Paull and Thierstein, 1987; Stoll and Ziveri, 2002) and the other is that based on microfiltration (Minoletti et al., ~~2008~~2009). The improvement of separation techniques offered a new perspective to study the Earth's history (e.g. Stoll, 2005; Beltran et al., 2007; Bolton and Stoll, 2013; Rousselle et al., 2013). Moreover, the development of coccolith oxygen and carbon isotope studies in culture in recent years (e.g. Ziveri et al., 2003; Rickaby et al., 2010; Hermoso et al., 2016; McClelland et al., 2017) has provided an improved mechanistic understanding of coccolith isotope data and therefore stimulated the need for more purified coccolith fraction samples from the fossil record.

Both decanting and microfiltering are widely used methods for coccolith separation. The m~~M~~icrofiltering method separates coccoliths with polycarbonate mirco-filter membrane ~~relies heavily on the specifications of micro filter membrane~~ (~~such as~~with pore sizes of 2µm, 3µm, 5µm ~~and~~ 8µm, 10µm and 12µm ~~pore size~~). ~~and~~ This method is highly effective in the larger size ranges, but is very time consuming in sediments with a high proportion of ~~very~~ small (<5µm) coccoliths (which tends to be the case in natural populations). It is also impossible to separate coccoliths with similar lengths by microfiltration, such as *Florisphaera profunda* and *Emiliania huxleyi* (Hermoso et al., 2015). Decanting, on the other hand, is highly effective for the small-sized coccoliths, because their slow settling times permit a greater ability to separate different sizes. Consequently, in some studies, a combination of the micro filtering and sinking or centrifugation method were applied for coccolith separation (Stoll, 2005; Bolton et al., 2012; Hermoso et al., 2015). The repeated

sinking/decanting method, first employed by (Edwards, 1963; Paull and Thierstein, 1987) follows the simple principle formalized by Stokes' Law for spherical particles: particles of larger size settle more quickly because they have a higher ratio of volume and mass (accelerating sinking) to sectional area (resistance retarding sinking). However, the sinking velocities of coccoliths with complex shape are difficult to calculate and have not been quantified in previous studies. Consequently, the repeated decanting method has generally used settling times based on empirical trial and error.

In ~~this~~ the current study, we present a novel and rigorous estimation of ~~the~~ sinking velocity for 16 species of modern and Cenozoic coccoliths, carefully measured in 0.2% ammonia at 20℃. With this new dataset, we explore how to estimate the sinking velocity of coccoliths based on their~~by~~ shape and length, which allows our estimations to be generalized for other species, and for situations where the mean ~~thickness~~ length of coccoliths of a given species was different from that of our study. These generalizations, together with our results on sinking velocities of one coccolith species (*Gephyrocapsa oceanica*) in different vessels, should allow a significant improvement in efficiency of future protocols for separation of coccoliths by repeated decanting.

2. Materials and methods

2.1 Sample selections

We measured the sinking velocity of 16 different species of coccoliths,~~–~~ isolated from eight deep-sea sediment samples from the Pacific and Atlantic Oceans (Figure 1, Table A1). Sample were principally of Quaternary age but ~~, including~~include two Neogene/Paleogene samples ~~(Figure 1)~~. In general, n~~N~~umbers of small coccoliths, including *E. huxleyi*, *Gephyrocapsa* spp and *Reticulofenestra* spp. are about an order of magnitude greater than that of larger coccoliths. However, the larger coccoliths' contributions to carbonate can be as high as 50% (Baumann, 2004; Jin et al., 2016). Moreover, both small coccoliths and large coccoliths are useful in geochemical analyses (Ziveri et al., 2003; Rickaby et al., 2010; Candelier et al., 2013; Bolton et al., 2012, 2016; Bolton and Stoll, 2013). Therefore, both small and large coccoliths were studied in this research. ~~The coccoliths were isolated from eight samples from the Pacific and Atlantic Oceans (more location information are in Figure 1 and Table A1; the pictures of studied coccolith can be found in Appendix B).~~ ~~All~~ Pictures of the studied coccolith are shown in Appendix B, and all classifications ~~of coccolith~~

follow Nannotax3 except *Reticulofenestra* spp. (Figure C2 in Appendix C).

2.2 Experiment designs

2.2.1 Sample pretreatments

The sinking velocity measurement depends on absolute abundance estimation (more details in 2.2.2). However, on microscope slides, larger coccoliths and foraminifer fragments may cover smaller coccoliths, reducing the accuracy of coccolith absolute numbers. Thus, before sinking experiments were carried out, raw sediments were pretreated to purify the target coccoliths to reduce errors in coccolith counting. The raw sediments were disaggregated in 0.2% ammonia and sieved through a 63 μm sieve and then treated by sinking method or filtering method (Bolton et al., 2012; Minoletti et al., ~~2008~~2009) to concentrate the target species up to at least more than 50% of the total assemblage~~s~~ (for Noëlaerhabdaceae coccoliths, a percentage more than 90% can be easily achieved). In one sample with aggregation (ODP 807), we did a rapid settling (30 min, 2 cm) to eliminate aggregates. Most of the species were measured individually in settling experiments, except ~~the~~ for *Pseudoemiliania lacunosa* and *Umbilicosphaera sibogae*, which ~~cannot be separated from each other~~were measured together.

2.2.2 Measuring the sinking speeds of coccoliths

We are not aware of any prior direct determination of the sinking velocity of individual coccoliths, although the sinking velocities of live coccolithophores and other marine ~~algae~~algal cells have been successfully measured by the 'FlowCAM' method (Bach et al., 2012) or a similar photography technique (e.g. Miklasz and Denny, 2010). Here we introduce a simple method to measure the particle sinking speeds without special equipment.

1. After pretreatment, the coccolith suspensions were gently shaken and then moved into comparison tubes which were vertically mounted on tube shelves. We set the timer going and let the suspension settle for a specified period of time, marked as sinking time or settling duration (T);~~.~~
2. Thereafter, we removed the upper 15 ml supernatant into a 50 ml centrifuge tube with a 10 ml pipette. This operation ~~should be~~was performed slowly and gently to avoid drawing lower suspensions upward. The absolute counting of cocolith was achieved by using the 'drop technique' to make quantitative microscope sides (Koch and Young, 2007; Bordiga

Formatted: Font color: Text 1

Formatted: List Paragraph, Numbered + Level: 1 + Numbering Style: 1, 2, 3, … + Start at: 1 + Alignment: Left + Aligned at: 0.63 cm + Indent at: 1.27 cm

Formatted: Font color: Text 1

Formatted: Font color: Text 1

et al., 2015). 0.3 ml mixed suspension was extracted and pipettes onto a glass cover and dry the slider on a hotplate;

3. The lower suspension was than to homogenized and another slider was prepare as described above;

4. The number of coccoliths in the upper and lower suspensions were carefully counted ~~by the 'drop technique'~~ on microscope at ×1250 magnification and the number of coccoliths and fields of view (FOV) were recorded for further calculations. ~~, which is a quick method to determine absolute abundance of coccoliths (Koch and Young, 2007; Bordiga et al., 2015).~~ More than 300 specimens were counted for most of the measurements. For the *Helicosphaera carteri* measurements, more than 100 FOV were checked and about 100 specimens were counted.

To calculate the sinking velocities of coccoliths, we define a parameter named the separation ratio (R), which represents the percentage of removed coccoliths in one separation by pumping out the upper suspension. This parameter is important and will be repeatedly mentioned in the following part. R was measured using the following equation (more details about derivation can be found in Appendix D):

$$R = \frac{\frac{N_1}{n_1}\times V_1 \sout{V_1}}{\frac{N_1}{n_1}\times V_1 \sout{V_1} + \frac{N_2}{n_2}\times V_2 \sout{V_2}} \quad (2\text{-}1)$$

where N_1 and N_2 are numbers of coccoliths counted in upper and lower suspension slides, respectively; n_1 and n_2 are the number of ~~fields of view (~~FOV~~)~~ counted. V_1 and V_2 are the volume of the settling vessel defined by the settling distance, as shown in Figure 2.

The separation ratio, R, also has a relationship with sinking time, T (Appendix D):

$$R = \frac{V_1 - \frac{V_1}{D}\times \sout{s}v\times T}{V_1+V_2} \quad (2\text{-}2)$$

where V_1, V_2 and D are shape parameters shown in Figure 2; and ~~sv~~ v is the average sinking velocity of measured coccoliths. If we plot R against T, the slope of line has a relationship with ~~s~~v. ~~Hence~~ Then liner regressions between R and T were processed with MATLAB to calculate the ~~s~~v (details about error analyses can be found in Appendix E).

There are still two issues to be explained. ~~The first one~~Firstly, ~~is~~ to eliminate the shape differences among vessels, all separation ratios have been transferred to calibrated separation ratios (R_{cal}), which means the separation ratio measured in a standard vessel with V_1=15 ml, V_2=10 ml and D=6 cm

Formatted: Font color: Text 1
Formatted: Font color: Text 1
Formatted: Font: Italic
Formatted: Font color: Text 1
Formatted: Subscript
Formatted: Subscript
Formatted: Subscript
Formatted: Subscript
Formatted: Subscript
Formatted: Subscript
Formatted: Subscript
Formatted: Subscript
Formatted: Subscript
Formatted: Subscript
Formatted: Subscript

(more details about transformation from R to R_{cal} can be found in Appendix D). ~~The other one is that~~Secondly, we treated the average sinking velocities as the sinking velocities of the coccoliths with the average length. This approximation has been proved reasonable in Appendix D.

Formatted: Subscript

2.2.3 Detecting the potential influence of vessels

Seven commonly used vessels were selected to detect the potential influence of vessels (Figure 3). Two of them are made of plastics (No.2 and No.3 in Figure 3) and all others are pyrex glass vessels. About 500 mg of sediment from ~~the~~ core KX21-2 were pretreated as described in 2.2.1 and suspended in about 500 ml ammonia. After that, settling experiments were performed as described in 2.2.2 using different vessels. In these experiments, only the dominant species, *G. oceanica*, was measured.

2.2.4 Other factors influencing the sinking velocity

Temperature can change the density and viscosity of liquid. Generally speaking, the higher the temperature is, the lower the density and viscosity will become and the faster pellets will sink. Take water for instance, if the temperature increases from 15 to 30℃, the particle sinking velocity will increase by ~43% (Table 1). All sinking velocities measured or discussed in the following sections were velocities at 20℃ to minimize the influence of temperature.

The calibration of sinking velocity in high concentration suspension has been calculated by Richardson and Zaki (1954)

$$~~s~~v = ~~s~~v_0(1-\alpha_s)^{2.7} \quad (2\text{-}3)$$

where the α_s is the solids volume fraction. Based on equation 2-3, the higher the suspension concentration is, the slower the sinking velocity will be. That is so called 'hindered settling'. When the α_s=0.2%, the reduction of sinking velocity owing to hindered settling is negligible ~~cannot be neglectable~~ (~~s~~v/~~s~~v_0 equals 99.46%). Hence, in this study all suspensions have solid volume fractions lower than 0.2% to avoid notable reductions of coccolith sinking velocities.

3. Results and Discussions

3.1 Influence of vessels

The sinking velocities of *G. oceanica* in the core KX21-2 in 0.2% ammonia at 20℃ measured in different vessels vary from 0.99 to 1.23 cm h^{-1}. The lowest value occurred in the 100 ml centrifuge

tube and the highest sinking velocity was measured in the 50 ml centrifuge tube experiments. The correlations between sinking velocities and different vessel parameters are quite low: r=0.13 for the vessel inner diameter, r=0.0005 for the sinking distance and r=0.051 for the upper volume and total volume ratio ($V_1/(V_1+V_2)$). The dissipation of energy by friction between the moving fluid and the walls can cause a reduction of sinking speed (wall effect). A significant wall effect will be detected when a particle is settling in a vessel ~~which~~ with a diameter that is smaller than the particle size by two orders of magnitude (Barnea and Mizarchi, 1973). The length of coccoliths is on the micron scales, so the diameters of vessel used in laboratory are ~~about~~ more than ~~three~~ four orders of magnitude larger than coccoliths. Moreover, our results show that the difference between vessel materials, glass and plastics, can also be ignored (Figure 4). Hence, we suggest that vessel type almost has no significant influence on sinking velocity of coccoliths.

However, our experiments were premised on the basis that the concentration of suspension was equal among different vessels. This means that large vessels can treat more sediment at one time but if we choose a larger vessel, more suspensions should be pumped and it often costs more time in sinking (often due to longer sinking distance). Assuming that the sediment is composed of 50% calcite (with density of 2.7 g cm^{-3}) and 50% clay (about 1.7 g cm^{-3}), the largest amount of sediment that can be used without significant reduction of the sinking velocity (5%) is about 400 mg in 100 ml suspension (this calculation is based on equation 2-3). However, because~~the~~ sediments ~~accumulating~~ accumulate in the lower suspension, the particle concentration can be more than 4 times higher than in the initial homogenous concentration. This phenomenon will be more significant for a vessel with a narrow bottom, such as centrifuge tubes. To avoid this, we recommend using about 100 mg dry sediment ~~should be~~ suspended in at least 100 ml suspension to avoid 'hindered settling'. If more sediment is necessary for geochemistry analyses, then a larger vessel should be selected to separate enough sample ~~in~~ at one time.

3.2 Sinking velocities at 20℃ in 0.2% ammonia

We measured the separation ratios of different coccoliths in comparison tubes at 20℃ in 0.2% ammonia (Figure 5). The sinking velocities of coccoliths were then calculated by linear fitting of separation ratios and settling durations. The sinking velocities of studied coccoliths vary by ~~one~~ two orders of magnitude from 0.154 cm h^{-1} to 10.67 cm h^{-1} (Table 2). The highest sinking velocity was

Formatted: Subscript
Formatted: Subscript
Formatted: Subscript

found in the measurement of *Coccolithus pelagicus* and the lowest velocity was found for *F. profunda*. The average sinking speed~~s~~ of coccolith~~s~~ is about 10-50% of the terminal sinking velocities of calcite spheres calculated by Stokes' Law (Figure 6~~c~~). These ratios are comparable ~~with the~~to the oval objects (e.g. seeds) data from Xie and Zhang (2001) and smaller than steel ellipsoids ~~those~~ data from McNown and Malaika (1950). The sinking velocities of coccoliths measured in our experiment are about 2-3 orders of magnitude smaller than values from sediment traps of 143-243 m d^{-1} (595~1012 cm h^{-1}) in the North Atlantic (Ziveri et al., 2000 and Stoll et al., 2007), ~~confirming~~ suggesting ~~the fact~~ that the coccoliths sinking out of the euphotic layer are mainly in the form of sinking aggregates rather than individual coccoliths.

3.3 Estimating the sinking velocities

Generally speaking, the sinking velocities of coccoliths increase with ~~the~~ distal shield length (Figure 5a), as expected from the increase in volume to sectional area for a given geometry as length increases. Our data implies that the sinking velocity has a power function relationship with distal shield length.

We propose that the sinking velocity of coccoliths might have a quadratic relationship with distal shield length as described by Stokes' Law (Figure 6a). If we use data for all species except ~~*Helicosphaera* *H.* *carteri*~~ ,(the reason can be found in the following discussion), the sinking velocities can be described by the following equation:

$$_{s}v = 0.0982\ (\pm 0.001)^{*}\ \phi^{2} \qquad (3\text{-}1)$$

Based on this quadratic regression, we derive a shape-velocity factor (k_{sv}) that relates settling velocity to coccolith length.

$$_{s}v = k_{sv}^{*}\ \phi^{2} \qquad (3\text{-}2)$$

Furthermore, this factor is analogous to the shape-mass factor, 'k_s' used to relate coccolith mass to coccolith length (Young and Ziveri, 2000). The length and shape-velocity factor of coccoliths can be used to predict most of the sinking velocity variations, however, variations may also arise due to changes in coccolith mass and thickness, for a given length, and due to the hydrodynamics of particular shapes. We noticed that the smaller coccolith *G. caribbeanica* has a greater sinking velocity than the larger coccolith, *G. oceanica*. We suggest that this was caused by greater mass per length (or greater average thickness) in the case of *G. caribbeanica* and this may be due to the closed

central area while *G. oceanica* has an open central area. Another example is *H. carteri*, ~~its~~ which lower~~smaller~~ sinking velocity of which can be explained by the unique structure of *H. carteri* coccolith ~~:~~. Firstly, the broad edge of *H. carteri* can increase the drag force significantly. ~~and *H. carteri* has the largest ellipticity (major axis length and minor axis length ratio) among the measured coccoliths, which means the mass of *H. carteri* is smaller than other species of coccoliths with similar lengths (Figure 6d and Figure C3).~~ Moreover, most of the measured coccoliths have a ellipticity (major axis length and minor axis length ratio) larger than 0.8, while the ellipticity of *H. carteri* is around 0.6, which means the mass of *H. carteri* is smaller than other species of coccoliths with similar lengths (Figure 6d and Figure C3). That is also the reason *H. carteri* was excluded from the general regression in equation 3-1. In the case of partial dissolution, the well-preserved *Cyclicargolithus floridanus* may have higher mass than dissolved (or disarticulated) *Cy. floridanus*, and therefore a slightly higher shape-velocity factor.

4. ~~Conclusions~~Suggestions for coccolith velocity estimations and separations

To improve coccolith separation by settling methods, we measured sinking velocities of different coccoliths by gravity. Sinking velocities in this study varied from 0.154 to 10.61 cm h^{-1}, about 10% to 50% of those of calcite spheres with same diameter. The shape of different vessels had little impact on the sinking velocity. But we should consider the volume of vessels to avoid 'hindered settling'. The sinking velocities are mainly controlled by the shape of coccolith, including the distal shield length, the size of central area, and the ellipticity of coccoliths. Besides the shape of coccoliths, temperature is also crucial to the coccolith separations because of the dependence of sinking velocities on temperature. Length-velocity factors were proposed to estimate coccoliths sinking velocities, so coccolith ~~sinking speeds in different samples can be easily estimated~~separation can be achieved by following steps:

1) Measure the ~~mean~~ length ~~–~~ of coccoliths in your target assemblage under the microscope and regress the length distribution by the assumption of normal distribution (details are in Appendix C);
2) Estimate sinking velocities for each important species. For species which ~~–~~ sinking speed has been directly measured, we can use the length-velocity factor directly ($v=k_v * \phi^2$). For unmeasured species, we can choose the length-velocity factor of coccoliths

Formatted: Font: Italic

Formatted: Font: Italic

Formatted: Font: Not Italic

Formatted: Numbered + Level: 1 + Numbering Style: 1, 2, 3, … + Start at: 1 + Alignment: Left + Aligned at: 1.27 cm + Indent at: 1.9 cm

with similar morphology in this study or use the general length-velocity formula ($v=0.098(\pm 0.001)* \phi^2$);

3) Calculate the separation time for main species. For example, in KX21-2 there are three main coccoliths, *F. prounda*, *G. oceanica* and *Ca. leptoporus* and we wish to separate *G. oceanica* out from the bulk sediment. Calculate each cocoliths' sinking velocity distributions as described in Step 2 above. As shown in Figure 7, a sinking velocity intermediate between *F. profunda* (with a length 2σ larger than average, marked as +2σ) and G. oceanica (with a length 2σ smaller than average, marked as -2σ) optimal to separate them, would be 0.6 cm h^{-1}. Similarly, we can chose speed thresholds 1.85 cm h^{-1} to separate *G. oceanica* from *Ca. leptoporus*. If we settle in a 50 ml centrifuge tube with a sinking distance, D, equal to 5.84 cm, the sinking time for separating *F. profunda* should be T=5.84/0.6=9.73 h. Similarly, we can calculate the time for separating *G. oceania* by T=5.84/1.85=3.16 h;

4) Homogenize the sediment suspension and let coccoliths settling as the period calculated in Step 3. After that, pump out the upper part of suspension. In the upper part, we have exclusively the smaller of the main coccoliths. However, column will still contain some smaller ones. So this step (settling and pumping) should be repeated until the lower part no longer has significant contribution from the smaller coccoliths. This step has been well described in pervious studies and more details can be found in Stoll and Ziveri (2002) and Bolton et al. (2012).

We find, i~~I~~f we use the general formula, ~~it should be noted that~~ a closed central area coccolith will sink faster than prediction (for *G. caribbeanica* and small *Ca. leptoporus* will settle ~40% faster) and coccoliths with greater ellipticity can settle much slower (for *H. carteri* will settle as 30% of the predicted sinking velocity for coccolith with similar length). Moreover, the sinking method cannot separate every species of coccoliths perfectly. As mentioned in Section 2.2.1, *P. lacunosa* and *U. sibogae* cannot easily be separated from each other because they have similar sinking velocities. Nevertheless, this study provides the first direct estimation of coccolith settling velocities, which should simplify implementation of future methods to separate coccoliths by settling time.

Formatted: Font: Italic
Formatted: Font: Italic
Formatted: Font: Italic
Formatted: Font: Italic
Formatted: Font: Italic
Formatted: Superscript
Formatted: Font: Italic
Formatted: Font: Italic
Formatted: Font: Italic
Formatted: Font: Italic
Formatted: Font: Italic
Formatted: Font: Italic

Acknowledgements. This study was supported by grants from the Chinese National Science Foundation (91428310, 91428309 and 41530964, to L.C.). We thank the Integrated Ocean Drilling Program (IODP) for providing the samples. The IODP is sponsored by the U.S. National Science Foundation and participating countries under management of the IODP Management International, Inc (IODP-MI).

Table 1. The influence of temperature on sinking velocity. Density data is from Kell (1975) and viscosity data is from Joseph et al. (1978).

T (℃)	ρ (g cm^{-3})	η (mPa s)	~~SV~~V$_T$: ~~SV~~V$_{T=20}$
15	0.9991	1.1447	0.8804
20	0.9982	1.0087	1
25	0.9970	0.8949	1.1279
30	0.9956	0.8000	1.2627

Table 2. The sinking velocity and shape-velocity factor of different coccolith species: ϕ means the distal shield length of coccolith and St ϕ is the standard deviation of distal shield length; sv represents the sinking velocity; ~~sv~~v (95%-) and ~~sv~~v (95%+) represent the lower and higher limit of 95% confidence level, respectively. 'k_{sv}' represents the length-sinking velocity factor. The short name of coccolith can be found in the caption of Figure 4. The details of coccoliths length distribution are in Appendix C.

Species	**abb.**	**ϕ (μm)**	**St ϕ (μm)**	**sinking velocity (cm h^{-1})**	**~~S~~vv (95% -)**	**~~S~~vv (95% +)**	**k_{sv}**
F. profunda	Fp-WP	1.508	0.557	0.158	0.010	0.011	0.070
F. profunda	Fp-SCS	1.786	0.641	0.154	0.051	0.052	0.048
small *Reticulofenestra*	Ret (<4um)	2.454	0.509	0.848	0.354	0.416	0.141
E. huxleyi	Emi	2.512	0.469	0.853	0.054	0.064	0.135
Gephyocapsa spp.	G spp	2.755	0.502	0.752	0.125	0.147	0.099
G. caribbeanica	Gcar	3.312	0.352	1.873	0.174	0.192	0.171
U. sibogae	Umb	4.060	0.500	1.268	0.416	0.441	0.077
G. oceanica	Geo	4.187	0.517	1.170	0.155	0.178	0.067
P. lacunosa	Pla	4.350	0.617	1.171	0.337	0.338	0.062
Small *Ca. leptoporus*	Cal small	4.605	0.629	3.351	0.172	0.199	0.158
large *Reticulofenestra*	Ret(>4um)	4.988	0.605	2.379	0.534	0.641	0.096
Cy. floridanus	Cyf	5.805	0.963	4.174	0.320	0.336	0.124
(dissolved) *Cy. floridanus*	Cyf -d	6.134	0.727	4.508	0.352	0.417	0.120
Large *Ca. leptoporus*	Cal large	6.370	0.931	3.737	1.053	1.336	0.092
H. carteri	Hel	8.936	0.994	2.541	1.740	2.440	0.032
Co. pelagicus	Cpl	10.640	1.175	10.610	0.950	1.235	0.094

Figure 1. Temporal and spatial distribution of samples. (a) The evolution of studied coccoliths: first occurrence and last occurrence data are from Nannotax3 (http://www.mikrotax.org/Nannotax3/index.html). The blue bars represent ranges of first occurrence and the green bars represent ranges of last occurrence. The blue diamonds represent samples used in this study. (b) Spatial distribution of samples. 1304 means IODP U1304, 3428 means MD12-3428cq, 1433 and 1435 means IODP U1433 and U1435, respectively. 807 means ODP 807 and 21-2 means KX21-2.

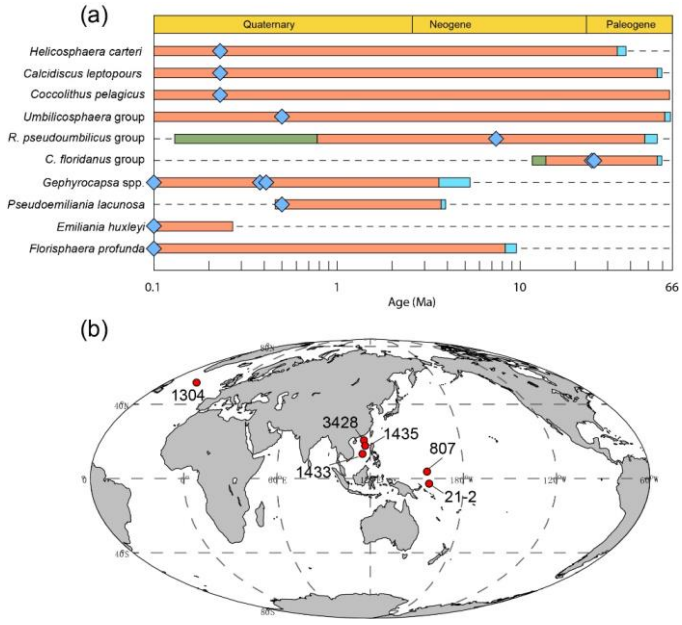

Figure 2. Schematic of settling experiments. ~~The pictures were taken after *Coccolithus pelagicus* sinking experiments with T=0 and T=30 min.~~ V_1 and V_2 are the volumes of the upper and lower cylinders, D is the settled distance. The numbers in circles are same as the number of Steps described in Section 2.2.1.

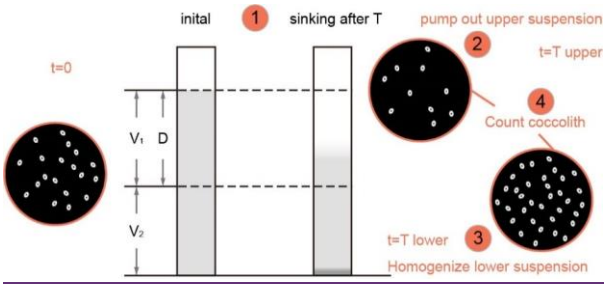

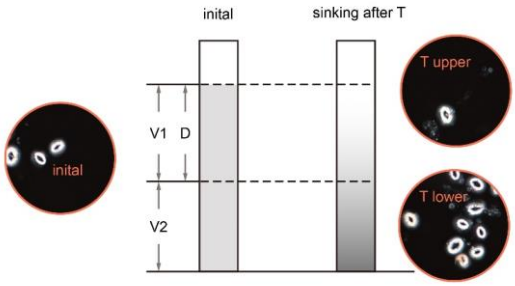

Formatted: Subscript

Formatted: Subscript

Figure 3. The shape parameters of vessels. V_1 and V_2 means the volume of upper suspension and lower suspension, respectively. D means sinking distance. Φ means average inner diameter which is calculated by $2*(V_1/(\pi D^3))^{1/2}$.

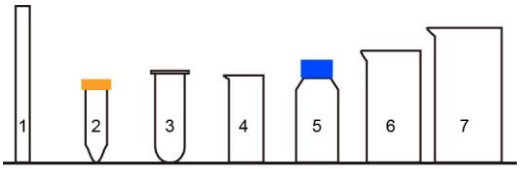

No.	Name	V1	V2	D (cm)	Φ (cm)
1	25 ml comparsion tube	15	10	6.376	1.73
2	50 ml centrifuge tube	30	20	5.480	2.64
3	100 ml centrifuge tube	50	30	4.854	3.62
4	100 ml beaker	40	40	2.834	4.24
5	100 ml reagent bottle	40	40	1.900	5.18
6	250 ml beaker	150	100	4.400	6.59
7	500 ml beaker	300	200	5.700	8.19

Formatted: Subscript
Formatted: Subscript
Formatted: Subscript
Formatted: Superscript

Figure 4. Sinking velocities of *G. oceanica* in the core KX-21-2 measured in different vessels. (a) The calibrated separation ratios measured in different vessels. Error bars show 95% confidence level of calibrated separation ratio. (b-d) The relationship between sinking velocity and different vessel shape parameters. Error bars represent 95% confidence level of sinking velocity in each vessel and the shade area represents 95% confidence level of sinking velocity considering all data points.

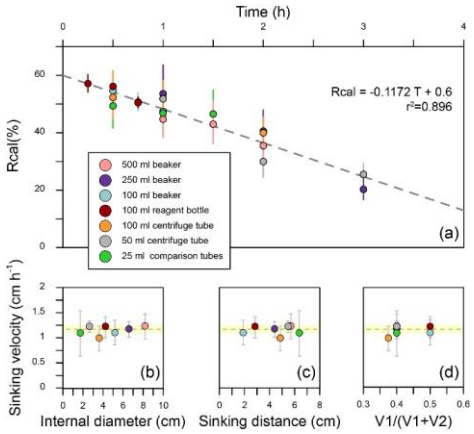

Figure 5. The calculated separation ratio (Rcal) vs sinking duration. Fp-WP means *F. profunda* in the West Pacific. Fp-SCS means *F. profunda* in the South China Sea. Emi means *E. huxleyi*. Gspp means small *Geophyocapsa*. Geo means *G. oceanica*. Gcarb means *G. caribbeanica*. Ret<4 means small *Reticulofenestra*. Ret>4 means large *Reticuloenestra*. Cyf means *Cyclicargolithus floridanus*. Cy-d means dissolved *Cy. floridanus*. Umb means *U. sibogae*. Pla means *Pseudo~~e~~miliania ~~lacunose~~lacunosa*. Hel means ~~*Helicosphaera*~~ *H. carteri*. Cal large means larger *Calicidiscus leptoporus*. Cal small means small *Ca. leptoporus*. Cpl means *Co. pelagicus*.

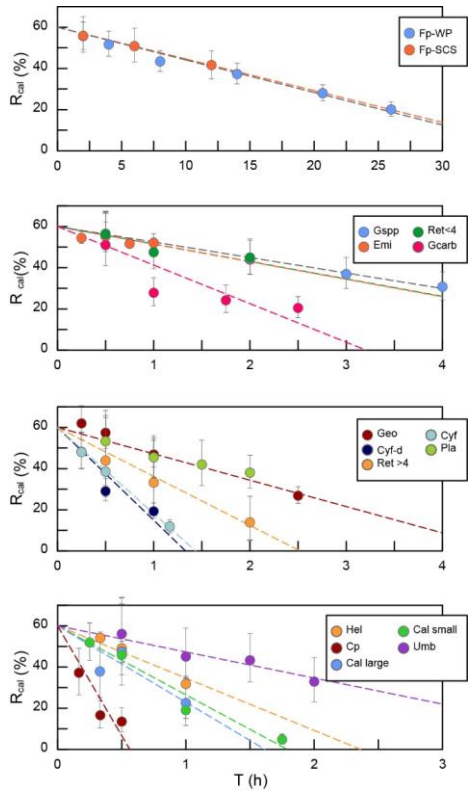

Figure 6. Coccolith sinking velocities and coccolith shape factors. (a-b) Sinking velocities and mean distal shield length. The horizontal error bars represent one standard deviation of coccolith length and the vertical ones represent 95% confidence level of measured sinking velocities. The blue, green and red lines represent sinking velocity of calcite sphere objects, coccolith sinking velocities estimated by Bolton et al. (2012) and this study, respectively. (c) The ratio of measured speed and speed calculated by Stokes' Law. (d) Coccolith short axis length (SAL) and long axis length (LAL) ratio against shape-velocity factor k_{sv}. Box shows median value and upper/lower quartiles, whiskers show maximum and minimum values, outliers larger than 1.5 of the interquartile range are shown as red crosses. The SAL against LAL plot was shown in Figure C3. The short names of coccoliths can be found in Table 2.

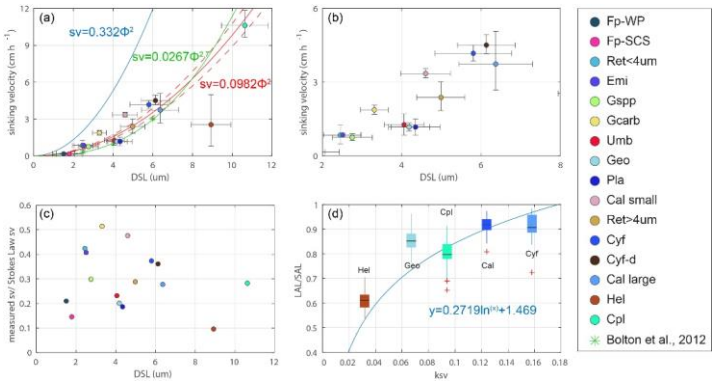

Figure 7. The selection of separation velocities: the sinking velocities of three main coccolith species in sample from core KX21-2 were calculated by the length distribution and velocity factors in Table 2. The yellow dots represent sinking velocities of coccoliths with mean length. The edge of boxes show the sinking velocities of coccolith within one standard deviation of length (±1σ) and the whiskers mark the sinking velocities of coccolith within two standard deviation of length (±2σ).

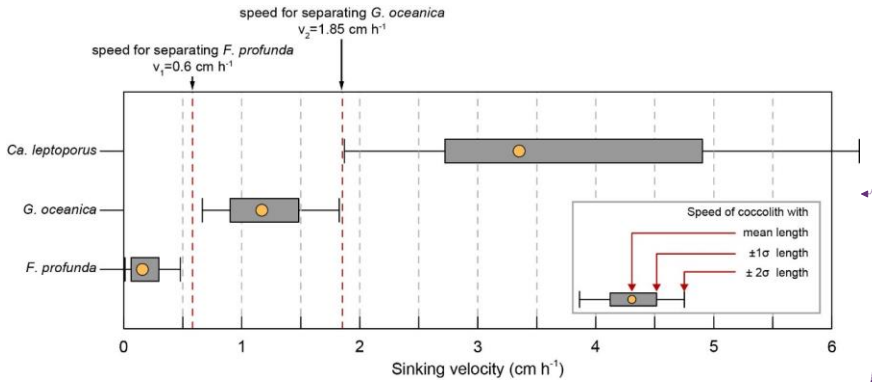

Formatted: Font: Bold

Formatted: Check spelling and grammar

Formatted: German (Switzerland)

Formatted: Normal

References

Bach, L.T., Riebesell, U., Sett, S., Febiri, S., Rzepka, P., Schulz, K.G., 2012. An approach for particle sinking velocity measurements in the 3-400 mum size range and considerations on the effect of temperature on sinking rates. Mar Biol 159, 1853-1864, doi:10.1007/s00227-012-1945-2.

Barnea, E., Mizrahi, J., 1973. A generalized approach to the fluid dynamics of particulate systems: Part 1. General correlation for fluidization and sedimentation in solid multiparticle systems. The Chemical Engineering Journal 5, 171-189, doi:10.1016/0300-9467(73)80008-5.

Baumann, K.-H., 2004. Importance of size measurements for coccolith carbonate flux estimates. Micropaleontology, 35-43.

Beaufort, L., Lancelot, Y., Camberlin, P., Cayre, O., Vincent, E., Bassinot, F., Labeyrie, L., 1997. Insolation cycles as a major control of equatorial Indian Ocean primary production. Science 278, 1451-1454, doi:10.1126/science.278.5342.1451.

Beltran, C., de Rafélis, M., Minoletti, F., Renard, M., Sicre, M.A., Ezat, U., 2007. Coccolith $\delta^{18}O$ and alkenone records in middle Pliocene orbitally controlled deposits: High-frequency temperature and salinity variations of sea surface water. Geochemistry, Geophysics, Geosystems 8, Q05003, doi:10.1029/2006GC001483.

Bolton, C.T., Hernandez-Sanchez, M.T., Fuertes, M.A., Gonzalez-Lemos, S., Abrevaya, L., Mendez-Vicente, A., Flores, J.A., Probert, I., Giosan, L., Johnson, J., Stoll, H.M., 2016. Decrease in coccolithophore calcification and CO2 since the middle Miocene. Nat Commun 7, 10284, doi:10.1038/ncomms10284.

Bolton, C.T., Stoll, H.M., 2013. Late Miocene threshold response of marine algae to carbon dioxide limitation. Nature 500, 558-562, doi:10.1038/nature12448.

Bolton, C.T., Stoll, H.M., Mendez-Vicente, A., 2012. Vital effects in coccolith calcite: Cenozoic climate-pCO2drove the diversity of carbon acquisition strategies in coccolithophores, Paleoceanography 27, doi:10.1029/2012pa002339.

Bordiga, M., Bartol, M., Henderiks, J., 2015. Absolute nannofossil abundance estimates: Quantifying the pros and cons of different techniques. Revue de micropaléontologie 58,

155-165 doi:10.1016/j.revmic.2015.05.002.

Candelier, Y., Minoletti, F., Probert, I., Hermoso, M., 2013. Temperature dependence of oxygen isotope fractionation in coccolith calcite: A culture and core top calibration of the genus Calcidiscus. Geochimica et Cosmochimica Acta 100, 264-281, doi:10.1016/j.gca.2012.09.040.

Hermoso, M., Candelier, Y., Browning, T.J., Minoletti, F., 2015. Environmental control of the isotopic composition of subfossil coccolith calcite: Are laboratory culture data transferable to the natural environment? GeoResJ 7, 35-42, doi:10.1016/j.grj.2015.05.002.

Hermoso, M., Chan, I.Z.X., McClelland, H.L.O., Heureux, A.M.C., Rickaby, R.E.M., 2016. Vanishing coccolith vital effects with alleviated carbon limitation. Biogeosciences 13, 301-312, doi:10.5194/bg-13-301-2016.

Jin, X., Liu, C., Poulton, A.J., Dai, M., Guo, X., 2016. Coccolithophore responses to environmental variability in the South China Sea: species composition and calcite content. Biogeosciences 13, 4843-4861, doi: 10.5194/bg-13-4843-2016.

Kell, G.S., 1975. Density, thermal expansivity, and compressibility of liquid water from 0. deg. to 150. deg.. correlations and tables for atmospheric pressure and saturation reviewed and expressed on 1968 temperature scale. Journal of Chemical and Engineering Data 20, 97-105.

Kestin, J., Sokolov, M., Wakeham, W.A., 1978. Viscosity of liquid water in the range −8 °C to 150 °C. Journal of Physical and Chemical Reference Data 7, 941-948.

Koch, C., Young, J., 2007. A simple weighing and dilution technique for determining absolute abundances of coccoliths from sediment samples. J. Nannoplankton Res.

McClelland, H.L., Bruggeman, J., Hermoso, M., Rickaby, R.E., 2017. The origin of carbon isotope vital effects in coccolith calcite. Nat Commun 8, 14511, doi:10.1038/ncomms14511.

McClelland, H.L., Barbarin, N., Beaufort, L., Hermoso, M., Ferretti, P., Greaves, M., Rickaby, R.E.M., 2016. Calcification response of a key phytoplankton family to millennial-scale environmental change. Scientific Reports 6, 34263, doi: 10.1038/srep34263.

McNown, John S., and Jamil Malaika. "Effects of particle shape on settling velocity at low

Reynolds numbers." Eos, Transactions American Geophysical Union 31.1 (1950): 74-82.

Miklasz, K.A., Denny, M.W., 2010. Diatom sinkings speeds: Improved predictions and insight from a modified Stokes' law. Limnology and Oceanography 55, 2513-2525, doi:10.4319/lo.2010.55.6.2513.

Minoletti, F., Hermoso, M., Gressier, V., ~~2008~~2009. Separation of sedimentary micron-sized particles for palaeoceanography and calcareous nannoplankton biogeochemistry. Nat. Protocols 4, 14-24, doi:10.1038/nprot.2008.200.

Paull, C.K., Thierstein, H.R., 1987. Stable isotopic fractionation among particles in Quaternary coccolith-sized deep-sea sediments. Paleoceanography 2, 423-429, doi:10.1029/PA002i004p00423.

Edwards, A.R., 1963. A preparation technique for calcareous nannoplankton. Micropaleontology 9, 103-104.

Richardson, J., Zaki, W., 1954. The sedimentation of a suspension of uniform spheres under conditions of viscous flow. Chemical Engineering Science 3, 65-73.

Rickaby, R.E.M., Henderiks, J., Young, J.N., 2010. Perturbing phytoplankton: response and isotopic fractionation with changing carbonate chemistry in two coccolithophore species. Clim. Past 6, 771-785, doi:10.5194/cp-6-771-2010.

Rousselle, G., Beltran, C., Sicre, M.-A., Raffi, I., De Rafélis, M., 2013. Changes in sea-surface conditions in the Equatorial Pacific during the middle Miocene–Pliocene as inferred from coccolith geochemistry. Earth and Planetary Science Letters 361, 412-421, doi:10.1016/j.epsl.2012.11.003.

Sprengel, C., Baumann, K.-H., Henderiks, J., Henrich, R., Neuer, S., 2002. Modern coccolithophore and carbonate sedimentation along a productivity gradient in the Canary Islands region: seasonal export production and surface accumulation rates. Deep Sea Research Part II: Topical Studies in Oceanography 49, 3577-3598 doi: 10.1016/S0967-0645(02)00099-1.

Stoll, H.M., 2005. Limited range of interspecific vital effects in coccolith stable isotopic records during the Paleocene-Eocene thermal maximum. Paleoceanography 20, doi:10.1029/2004pa001046.

436 Stoll, H.M., Rosenthal, Y., Falkowski, P., 2002. Climate proxies from Sr/Ca of coccolith calcite:
437 calibrations from continuous culture of Emiliania huxleyi. Geochimica et Cosmochimica
438 Acta 66, 927-936, doi:10.1016/S0016-7037(01)00836-5.
439 Stoll, H.M., Ziveri, P., 2002. Separation of monospecific and restricted coccolith assemblages
440 from sediments using differential settling velocity. Marine Micropaleontology 46, 209-
441 221, doi: 10.1016/S0377-8398(02)00040-3.
442 ~~Tremblin, M., Hermoso, M., Minoletti, F., 2016. Equatorial heat accumulation as a long-term~~
443 ~~trigger of permanent Antarctic ice sheets during the Cenozoic. Proceedings of the National~~
444 ~~Academy of Sciences 113, 11782-11787 doi: 10.1073/pnas.1608100113.~~
445 Xie, H-Y., and D-W. Zhang. "Stokes shape factor and its application in the measurement of
446 spherity of non-spherical particles." Powder Technology 114.1 (2001): 102-105 doi:
447 10.1016/S0032-5910(00)00269-2.
448 Young, J.R., Ziveri, P., 2000. Calculation of coccolith volume and it use in calibration of
449 carbonate flux estimates. Deep sea research Part II: Topical studies in oceanography 47,
450 1679-1700, doi:10.1016/S0967-0645(00)00003-5.
451 Zhang, H., Liu, C., Jin, X., Shi, J., Zhao, S., Jian, Z., 2016. Dynamics of primary productivity
452 in the northern South China Sea over the past 24,000 years. Geochemistry, Geophysics,
453 Geosystems 17, 4878-4891, doi:10.1002/2016GC006602 .
454 Ziveri, P., Stoll, H., Probert, I., Klaas, C., Geisen, M., Ganssen, G., Young, J., 2003. Stable
455 isotope 'vital effects' in coccolith calcite. Earth and Planetary Science Letters 210, 137-
456 149, doi:10.1016/S0012-821X(03)00101-8.

Appendix A. Sample selections

Table A1. Sample selections

Measured coccolith	abb.	Region	Core	Section	Epoch	Age model ref.
F. profunda	Fp-SCS	SCS	MD12-3428	0-1 cm	Holocene	Zhang et al., 2016
F. profunda	Fp-WP	W.P.	KX21-2	2-4 cm	Holocene	Liang et al., 2016
E. huxleyi	Emi	SCS	MD12-3428	0-1 cm	Holocene	Zhang et al., 2016
Gephyocapsa spp.	Gspp	W.P.	ODP 807A	1H 5W 102-104	Pleistocene	Jin et al., 2010
G. oceanica	Geo	W.P.	KX21-2	2-4 cm	Holocene	Liang et al., 2016
G. caribbeanica	Gcarb	N.A.	IODP 1304B	7H 5W 69-70	Pleistocene	Channell et al., 2010
small *Reticulofenestra*	Ret<4	SCS	IODP 1433B	28R 2W 30-34	Miocene	Li et al., 2013
large *Reticulofenestra*	Ret>4	SCS	IODP 1433B	28R 2W 30-34	Miocene	Li et al., 2013
Cyclicargolithus floridanus	Cyf	SCS	IODP 1435A	6R 3W 25-29	Oligocene	Li et al., 2013
Cyclicargolithus floridanus	Cyf-d	SCS	IODP 1435A	8R 1W 27-31	Oligocene	Li et al., 2013
Umbilicosphaera sibogae	Umb	W.P.	ODP 807A	3H 5W 92-94	Pleistocene	Jin et al., 2010
Pseudoemiliania lacunosa	Pla	W.P.	ODP 807A	3H 5W 92-94	Pleistocene	Jin et al., 2010
Helicosphaera carteri	Hel	W.P.	ODP 807A	3H 5W 92-94	Pleistocene	Jin et al., 2010
large *Calcidiscus leptoporus*	Cal large	W.P.	ODP 807A	3H 5W 92-94	Pleistocene	Jin et al., 2010
small *Calcidiscus leptoporus*	Cal small	N.A.	IODP 1304B	7H 5W 69-70	Pleistocene	Channell et al., 2010
Coccolithus pelagicus	Cpl	N.A.	IODP 1304B	7H 5W 69-70	Pleistocene	Channell et al., 2010

References:

Channell, J., Sato, T., Kanamatsu, T., Stein, R., Alvarez Zarikian, C., 2010. Expedition 303/306 synthesis: North Atlantic climate. Channell, JET, Kanamatsu, T., Sato, T., Stein, R., Alvarez Zarikian, CA, Malone, MJ, and the Expedition 303, 306.

Jin, H., Jian, Z., Cheng, X., Guo, J., 2011. Early Pleistocene formation of the asymmetric east-west pattern of upper water structure in the equatorial Pacific Ocean. Chinese Science Bulletin 56, 2251-2257.

Li, C.-F., Lin, J., Kulhanek, D.K., 2013. South China Sea tectonics: Opening of the South China Sea and its implications for southeastAsian tectonics, climates, and deep mantle processes since the late Mesozoic. IODP Sci. Prosp 349.

Liang, D., Liu, C., 2016. Variations and controlling factors of the coccolith weight in the Western Pacific Warm Pool over the last 200 ka. Journal of Ocean University of China 15, 456-464.

Zhang, H., Liu, C., Jin, X., Shi, J., Zhao, S., Jian, Z., 2016. Dynamics of primary productivity in the northern South China Sea over the past 24,000 years. Geochemistry, Geophysics, Geosystems 17, 4878-4891.

Appendix B. Coccolith images under circular polarized light

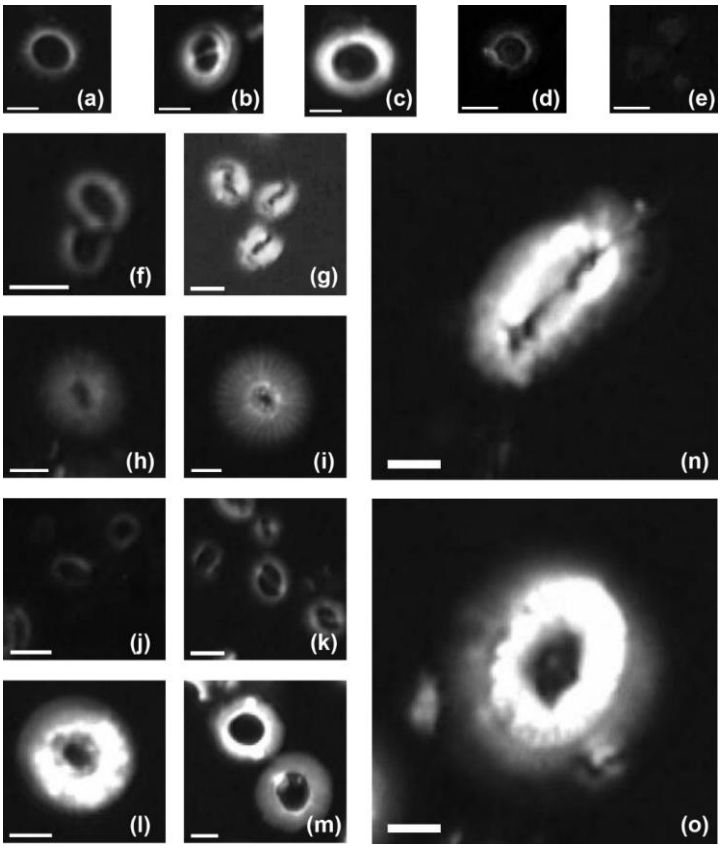

Plate B1. Imaged of measured coccolith in this study: (a) *Pseudoemiliania lacinosa* in the core ODP 807; (b) *Gephyrocapsa oceanica* in the core KX21-2; (c) *Reticulofenestra* spp. (large) in the core IODP U1433B; (d) *Umbilicosphaera sibogae* in the core ODP 807; (e) *Florispharea profunda* in the core KX21-2; (f) *Reticulofenestra* spp. (small) in the core IODP U1433B; (g) *Gephyrocapsa caribbeanica* in the core IODP U1304B; (h) small *Calcidiscus leptopourus* in the core IODP U1304B; (i) large *Calcidiscus leptopourus leptoporus* in the core ODP 807A; (j) *Emiliania huxleyi* in the surface sediment in the South China Sea; (k) *Gephyrocapsa* spp. in the core ODP 807; (l) *Cyclicargolithus floridanus* in the core IODP U1435A and (m) dissolved *Cyclicargolithus floridanus* in the same core; (n) *Helicosphaera carteri* in the core ODP 807A; (o) *Coccolithus pelagicus* in the core IODP U1304B. White bars represent a length of 2 μm.

Formatted: Font: Italic

Appendix C. The length distribution of coccoliths

To measure the distal shield length of coccoliths, pictures were taken at a magnification of 1250x under circular polarized light. The coccolith lengths were measured by using the image analysis software, ImageJ. More than 5 pictures were taken and more than 50 (usually more than 100) coccolith specimens were measured. The length distributions of coccoliths measured in our experiments were shown in the Figure C1.

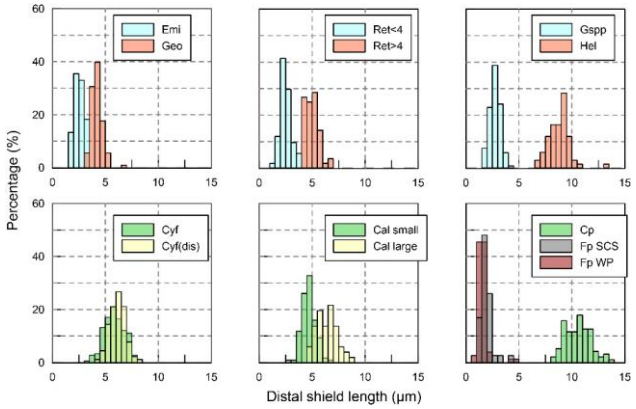

Figure C1. Size distribution of coccolith measured in the present study. The shorten names of coccolith follow Table A1.

The classification of coccoliths by length was supported by mixture analysis in PAST (Hammer et al., 2001), such as *Reticulofenestra* spp. and *Gephyrocapsa* spp. *Reticulofenestra* spp. in the Miocene were classified into two groups, Ret. (<4 μm) and Ret. (>4 μm). The traditional classification of *Reticulofenestra* spp. is <3 μm, 3-5 μm and 5-7 μm didn't pass the normal distribution test. Hence, in this study the *Reticulofenestra* spp. are divided at 4 μm (Figure C2). *Gephyrocapsa* spp. were classified by the shape of coccoliths into small *Gephyrocapsa* (central area opening and length <3.5 μm), *G. oceanica* (central area opening and length >3.5μm) and *G. caribbeanica* (closed central area) by the length and central area.

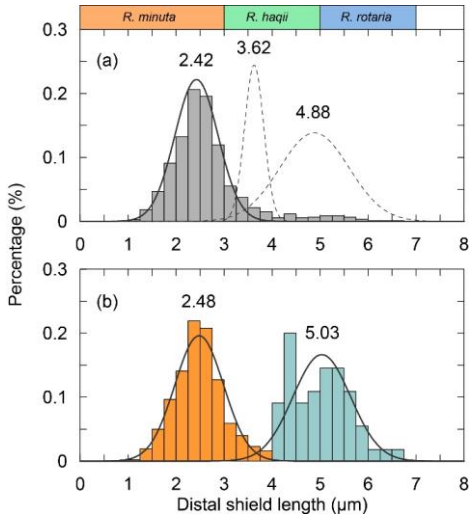

505

506 **Figure C2**. The classical classification of *Reticulofenestra* spp. (a) and the classification used in our
507 study (b). The curves represent the normal distribution fits of different coccolith groups and the dish
508 curve marks that the goodness of fit is below 0.2.

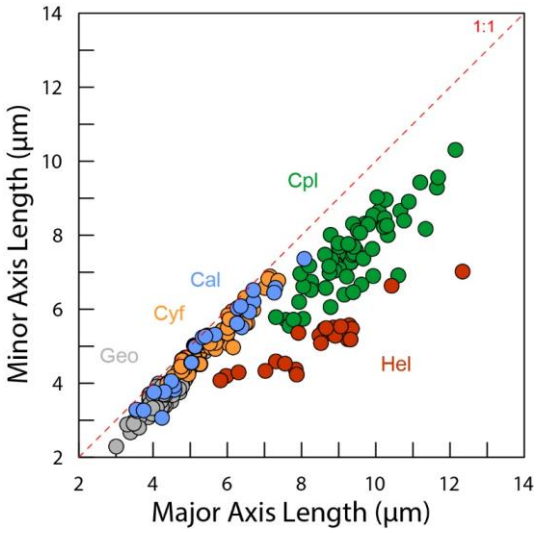

509

510 **Figure C3.** The short axis and long axis length distribution of coccoliths in Figure 6d.

511 **Reference.**

512 Hammer, Ø., Harper, D., Ryan, P., 2001. Paleontological Statistics Software: Package for
513 Education and Data Analysis. Palaeontologia Electronica.

Formatted: English (United States)

Appendix D. Coccolith movement in gravity settling

In this part, the derivation of equation will be explained in detail including proofs of several assumptions mentioned in the methods part.

When the well mixed sediment begins to sink, the decrease of coccoliths number in the upper suspension (N_u) can be described as following equation:

$$\frac{dN_u}{dT} = -\frac{N_{u(t=0)}}{D} \times sv \quad \text{(D-1)}$$

where the D is the length of upper suspension and $N_{u(t=0)}$ /D is the initial number of coccolith in cross-section with a unit thickness ~~of dD~~, v is the sinking velocity of coccolith.

Do integration for the equation D-1, we can get the variation of coccolith number in the upper column over time:

$$N_u = N_{u(t=0)} - \frac{N_{u(t=0)}}{D} \times sv \times T \quad \text{(D-2)}$$

where T is settling time. After a period of time (T), we pump out the upper suspension. Here we define the number of coccoliths in the upper supernatant dividing the total coccoliths number in the tube (N_t) as separation ratio (R), which represents the percentage of total coccoliths removed in one separation~~. This parameter is important and will be repeatedly mentioned in the following part~~. R can be expressed by

$$R = \frac{Nu}{Nt} \quad \text{(D-3)}$$

Assuming all coccoliths are uniformly distributed in the suspension at the beginning of settling, $N_{u(t=0)}$ has relationship with N_t as follow:

$$\frac{Nu(t=0)}{Nt} = \frac{V_1 V1}{V_1 V1 + V_2 V2} \quad \text{(D-4)}$$

where V_1 is the volume of upper suspensions and V_2 is the volume of lower suspensions.

Combining the equation D-1, D-2, D-3 and D-4, we obtain the relationship between separation ratio, R, and sinking velocity, ~~sv~~v, as follow:

$$R = \frac{N_u}{N_t} = \frac{N_{u(t=0)} - \frac{N_{u(t=0)}}{D} \times sv \times T}{N_t} = \frac{V_1 - \frac{V_1}{D} \times sv \times T}{V_1 + V_2} \quad \text{(D-5)}$$

If we plot the R and T on a figure, the slope of the line is a function of V_1, V_2, D and ~~sv~~v. Since the V_1, V_2, D are known parameters, we say the slope of R-T is a function of ~~sv~~v, which is exactly what we want.

Formatted: Subscript

Formatted: Subscript

Formatted: Subscript

Formatted: Subscript

Formatted: Subscript

Formatted: Subscript

Formatted: Subscript

Formatted: Subscript

Comparison tubes used in our experiments have the same V_1 and V_2 but different D. Other vessels used in other experiments have different V_1, V_2 and D. So we should adjust the raw separation ratio to calibrated separation ratio (R_{cal}), which represents the separation ratio made in a standard vessel with V_{1std}=15 ml, V_{2std}=10 ml and D_{std}=6 cm. This step can be described by equation ~~2~~D-6:

$$RR_{cal}\text{~~cal~~} = \frac{[R\times(V_1\text{~~V1~~}+V_1\text{~~V2~~})-V_1\text{~~V1~~}]\times D\times V_{1std}\text{~~15~~}}{(D_{std}\text{~~6~~}\times V_1\text{~~V1~~}+V_{1std}\text{~~15~~})\times(V_{1std}+V_{2std})\text{~~25~~}} \quad \text{(D-6)}$$

After calibrated, the slope of R_{cal}-T (k) has relationship with ~~sv~~ v as following equation:

$$\text{~~sv~~}v = -\frac{D_{std}\times(V_{1std}+V_{2std})}{V_{1std}}\text{~~10~~} \times k = -10 \times k \quad \text{(D-7)}$$

where k is the slope of R_{cal} against T from regression and other parameters are as described above. Hence, the sinking velocity of different coccoliths can be achieved by measuring the variations of R_{cal} over time.

The coccoliths' lengths in the sediment have some varations. So what we measured is actually the bulk settling velocity of whole coccolith population. We also offer a test for the assumption that the average sinking velocity of all coccoliths can be treated as the sinking velocity of coccoliths with the average length. Here we used the data of *G. oceanica*. A normal distribution was fitted to the measured length distribution (Figure D1-a). We generated 100000 coccolith following the normal distribution and let these coccolith evenly distributing in the comparison tube at the initial and then set them sinking without collisions with each other. ~~And then we simulate a normal distribution situation of coccoliths in the vessel.~~ The sinking velocities of different size coccoliths were calculated by the ~~cubic~~ velocity-shape parameter '~~b~~' k_v' as described in discussion part. We modeled the coccoliths sinking process and computed the separation ratio (red dash line in Figure D1-b), coccolith length (red dash line in Figure D1-c) and instant sinking velocities (orange dots in Figure D1-d) at different time sections.

Formatted: Subscript
Formatted: Subscript
Formatted: Subscript
Formatted: Subscript
Formatted: Subscript
Formatted: Subscript
Formatted: Subscript
Formatted: Subscript
Formatted: Subscript
Formatted: Subscript
Formatted: Subscript
Formatted: Font: Italic
Formatted: Subscript

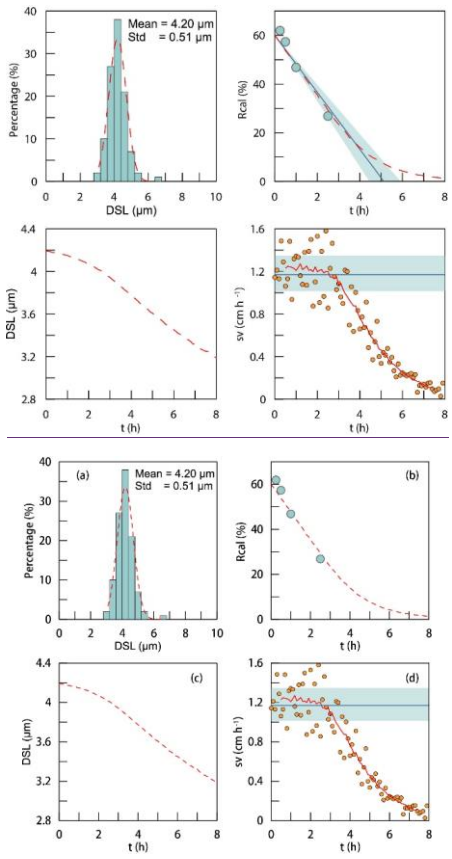

Figure D1. The simulations of coccoliths settling with different lengths: (a) the length distribution of coccoliths. The green bars represent measured data and red dash line represents the best fit for normal distribution. (b) The calibrated separation ratio: the green dots are measured data in our settling experiments, the blue line and shade area represent the calculated sinking velocity based on R_{cal} measurement and the red dash line represents results obtained from ~~Monte Carlo~~ simulations. (c) The average length of removed coccolith in simulations; (d) the modeling sinking velocities of coccoliths: the orange dots are instant sinking velocity calculated from derivation of R_{cal}, the red dash line is weighted average for the instant sinking velocity. Blue line represents the average sinking velocity we measured and the green shade area represents 95% confidence level of the measured velocity.

For *G. oceanica* experiments, the instant sinking velocity would not change significantly until settling for more 3 hours. That means for all R_{cal} larger than 15% are safe for liner regressions. The

Formatted: Font: (Default) Times New Roman, (Asian) Times New Roman

Formatted: Subscript

Formatted: Subscript

Formatted: Subscript

minimum safe number of R_{cal} will descend with the drop of dispersion degree of coccolith length distribution. Hence our assumption for average sinking velocity and the use of liner regression are proved to be reasonable.

Formatted: Subscript

Appendix E. Statistical and error analyses

The errors of measured separation ratio (R) and calculated sinking velocity (~~s~~v) are mainly caused by counting coccolith, the error of which fellows the Poisson distribution. To detect the influence of counting number on the result error, the error of separation ratio was simulated by 5000 times Monte Carlo calculations with assumptions that 'V_1:V_2=15:10' and 'n_1=n_2' (Figure E1). The result shows that the number of coccolith counted in the upper column draws more influence on the relative error ($|R-R_{95CL}|/R$). That means more coccolith in the upper suspension should be counted to make results more accurate. The slope of R_{cal}-T was calculated by liner fitting with the intercept fixed on $V_1/(V_1+V_2)$. The input R_{cal} were generated from measured values considering the error of coccolith counting. The ~~error of sinking velocity~~ regressions of R_{cal}-T ~~was also~~were repeated ~~calculated~~ by 5000 times ~~Monte Carlo simulations~~regressions in the software Matlab and the error of sinking velocity, v, was source from the distribution slope of R_{cal}-T in Monte Carlo process.

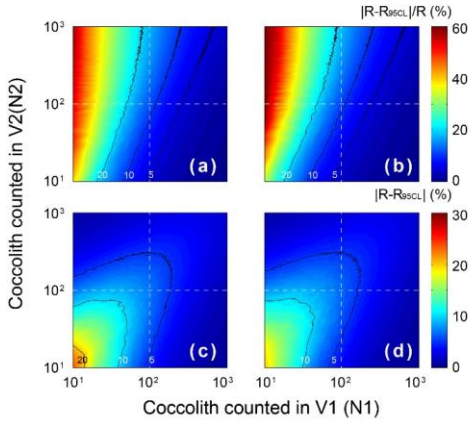

Figure E1. The error distribution with different N_1 and N_2 (ranging from 1 to 1000) simulated 5000 times by the Matlab with assumptions that the error distributions of N_1 and N_2 fellow Poisson distribution. The calculation of R follows equation 2-5, and here we assume numbers of FOV are equal (n_1=n_2). Counter lines mark values equal to 5, 10 and 20. (a) and (c) represent the lower 95% confidence level and (b) and (d) represent upper 95% confidence level. (a) and (b) the relative error of R and (c) and (d) represent the absolute error of R.

Formatted: Subscript
Formatted: Subscript
Formatted: Subscript
Formatted: Subscript
Formatted: Subscript
Formatted: Subscript
Formatted: Subscript
Formatted: Subscript
Formatted: Subscript
Formatted: Subscript
Formatted: Subscript
Formatted: Subscript
Formatted: Subscript
Formatted: Subscript
Formatted: Subscript
Formatted: Subscript